ISSN 0023-1584, Kinetics and Catalysis, 2009, Vol. 50, No. 5, pp. 627–635. © Pleiades Publishing, Ltd., 2009.
Original Russian Text © A.A. Paletsky, N.V. Budachev, O.P. Korobeinichev, 2009, published in Kinetika i Kataliz, 2009, Vol. 50, No. 5, pp. 653–662.

Mechanism and Kinetics of the Thermal Decomposition of 5-Aminotetrazole

A. A. Paletsky, N. V. Budachev, and O. P. Korobeinichev

Institute of Chemical Kinetics and Combustion, Siberian Branch, Russian Academy of Sciences, Novosibirsk, 630090 Russia
e-mail: korobein@kinetics.nsc.ru

Received July 1, 2008

Abstract—The kinetics of 5-aminotetrazole thermal decomposition in the condensed phase at high heating rates (~100 K/s) was studied by the dynamic mass spectrometric thermal analysis using a molecular beam sampling system, and the product composition was determined. Two routes of 5-aminotetrazole decomposition were distinguished, one yielding HN_3 and NH_2CN (route 1), and the other N_2 and CH_3N_3 (route 2). The activation energy and rate constant of 5-AT decomposition were determined for each route.

DOI: 10.1134/S0023158409050036

INTRODUCTION

5-Aminotetrazole (CH_3N_5, 5-AT), a promising energetic material with a high nitrogen content (82.3 wt %), is widely used in various gas generators. Due to its physicochemical properties (positive enthalpy of formation [1], thermal stability, and explosion safety), 5-AT is used in automotive safety pads [2], solid-fuel fire extinguishers [3, 4], and other applications as a source of environmentally friendly gaseous nitrogen, which results from the combustion of 5-AT-based mixtures. However, the self-sustained burning of pure 5-AT is possible only at high pressures [5, 6]. This makes it difficult to study 5-AT combustion chemistry by modern methods. The thermal decomposition of condensed substances is part of combustion process. Therefore, it is of great interest to study the thermal decomposition of 5-AT because knowledge of the mechanism of the thermal decomposition of such substances would contribute to the understanding of the processes that occur during their combustion.

The thermal decomposition of 5-AT was studied at different heating rates and under different pressures [7–12]. Under atmospheric pressure, 5-AT begins to decompose immediately after melting (~205°C [8]). Depending on the product removal conditions (blowing with an inert gas or decomposition in a closed space), 5-AT can decompose both without heat evolution and with evolution of a considerable amount of heat [8, 9]. At room temperature, 5-AT exists mainly in imino form (Fig. 1, structure **1**), which turns into amino form (Fig. 1, structures **2** and **3**) upon thermal treatment of the sample (melting or evaporation) [9, 10].

A mechanism of the thermal decomposition of 5-AT involving tautomeric forms of 5-AT and yielding gaseous (HN_3, N_2, NH_2CN, NH_3, HCN) and condensed (melamine (Fig. 1, structure **4**) and its forms) decomposition products was suggested [9, 10]. According to the scheme based on quantum chemical calculations, the formation of HN_3 can be due to the fragmentation of both the imino isomer (reaction (I)) and amino isomer (reactions (II) and (III)) of the 5-AT molecule. The decomposition of 5-AT yielding N_2 is possible only for the amino tautomeric forms of

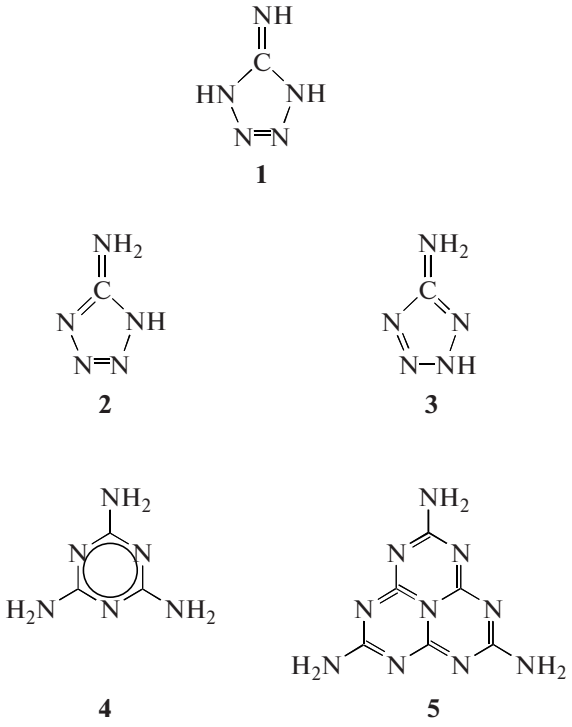

Fig. 1. Structural formulas of **1**, imino form of 5-AT; **2**, 1-H isomer of the amino form of 5-AT; **3**, 2-H isomer of the amino form of 5-AT; **4**, melamine; and **5**, melem.

5-AT molecules (reaction (IV) for the 1-H isomer of the amino form).

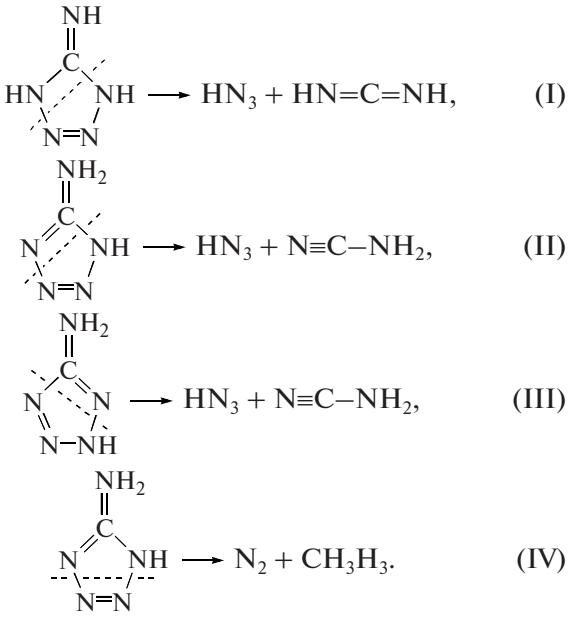

$$\xrightarrow{} HN_3 + HN{=}C{=}NH, \quad (I)$$

$$\xrightarrow{} HN_3 + N{\equiv}C{-}NH_2, \quad (II)$$

$$\xrightarrow{} HN_3 + N{\equiv}C{-}NH_2, \quad (III)$$

$$\xrightarrow{} N_2 + CH_3H_3. \quad (IV)$$

As was shown by IR spectroscopy and mass spectrometry (mass range from 14 to 44) [9], the major product of 5-AT thermal decomposition in a sealed ampule is HN_3, and N_2 and NH_3 were also detected. It was observed [8] that HN_3 appears upon 5-AT decomposition at ~210°C in an argon flow under a pressure of ~1 atm at high heating rates of ~100 K/s, which are higher than the heating rates used in [9] (~10 K/min). At ~260°C NH_2CN was detected in the gas phase. At a higher temperature, NH_3 was found at low concentrations as compared to those of HN_3 and NH_2CN.

According to [7–10], 5-AT decomposes via two parallel routes. The first route is the reaction 5-AT $\longrightarrow$ $HN_3 + NH_2CN$, which proceeds with the simultaneous splitting of two bonds in the tetrazole ring. The activation energy of this reaction was calculated to be ~200 kJ/mol [13]. The second route of the decomposition of the amino form of 5-AT (5-AT $\longrightarrow$ $N_2 + CH_3N_3$) is due to the splitting of the tetrazole ring and the formation of an intermediate structure, from which the nitrogen molecule is eliminated. The formation of this intermediate state (open tetrazole ring), as was shown by calculations [14], is the most important step determining the overall rate of the thermal decomposition of 5-AT. The activation energy of the formation of this intermediate state found by the quantum chemical calculation is 99.5 kJ/mol [14].

An analogy was drawn between the thermal decomposition of 5-AT and the fragmentation of the 5-AT molecule under electron impact mass spectrometric conditions, under which the above decomposition routes take place [15–17].

Two stages of 5-AT thermal decomposition were distinguished [9, 10] by thermogravimetry and IR spectroscopy at a heating rate of 0.63–60 K/min. About 50% of the initial weight of the sample was lost at the first stage of decomposition between 207 and 337°C. The absorption bands characteristic of the tetrazole ring disappeared completely at this stage. Thus, it can be assumed that only reactions involving the secondary products of 5-AT decomposition in the condensed phase occur at the extents of decomposition above 0.5. The activation energy (E_a) of 5-AT decomposition is a descending function of the extent of decomposition (x) [10]. The kinetic parameters of the first stage of 5-AT thermal decomposition obtained by three different data processing methods [10] are similar: $\sim E_a = 147 \pm 10$ kJ/mol and $\log k_0 = 13.1 \pm 1.0$ [s^{-1}].

Thus, as is clear from the literature, the kinetic studies of 5-AT thermal decomposition, including the calculation of the activation energy, did not address the quantitative analysis of the products resulting from decomposition via the different, simultaneously occurring routes.

The purpose of the present work is to study the kinetics and mechanism of the primary stages of the thermal decomposition of 5-AT using the dynamic mass spectrometric thermal analysis, including quantitative determination of the composition of the thermal decomposition products and calculation of the kinetic parameters of the primary stages of this process at heating rates higher than those used previously [10].

EXPERIMENTAL

The product composition and kinetics of 5-AT thermal decomposition were studied by dynamic mass spectrometric thermal analysis (DMSTA) using a molecular beam sampling system [18, 19]. An advantage of DMSTA over other methods is the possibility of determining the kinetic parameters of the decomposition of condensed substances with simultaneous identification of the resulting gaseous products. The sample injection method in the molecular beam mode makes it possible to sample both stable and labile substances (active species, atoms, radicals, and vapors of high-volatile substances) and to prevent the substances forming in heterogeneous reactions of the decomposition products on the hot walls of the probe from getting into the analyzer. An MSKh-4 time-of-flight mass spectrometer (Sumy, USSR) with a mass resolution of ~70 in the range of masses measured in this work (1–150 amu) was used as the analyzer. The mass spectrometer was operated in the external triggering mode with a frequency of 10 kHz and an ionizing electron energy of 70 eV.

The 5-AT powder used in experiments was prepared from 5-aminotetrazole monohydrate by drying [20] at 110°C for 24 h. The thermal decomposition of 5-AT was carried out in a flow reactor in an argon flow under a pressure of 1 atm. The reactor was a quartz tube with an internal diameter of 1 cm. Two series of experiments with different methods of sample deposition on the heater were carried out. In the first series,

a tungsten plate (variant 1) 0.1 mm × 2 mm × 20 mm in size was used as the heater. The plate was placed inside the flow reactor as described in [18]. A solution of 5-AT in ethanol was applied to the lateral surfaces of the central part of the plate. After the alcohol evaporated, the weight of the deposited sample was about 1–1.2 mg. The absence of water in the samples was checked by mass spectrometry, measuring the m/e = 18 (H_2O) peak intensity.

In the second experimental series, the heater was a tantalum foil boat (variant 2) ~0.037 cm^3 in volume. The powdered 5-AT sample was placed inside the boat. The crystal size in the powder was about 20 μm, the sample weight was ~1 mg, and the bulk density of the powder was 0.2 g/cm^3. In this case, the thermal decomposition of 5-AT was carried out in two variants: (1) mass spectrometric measurements and (2) measurements of the temperature of the decomposition products in the gas phase using a thermocouple. It should be mentioned that the latter measurements were qualitative and were performed to monitor the ignition of 5-AT during its thermal decomposition. The results of these experiments were not used in the calculation of the kinetic parameters of thermal decomposition because of the insufficiently correct measurement of the sample temperature at high heating rates (loose thermal contact between the bulk 5-AT powder and the substrate). A tungsten–rhenium thermocouple 30 μm in diameter was mounted in the gas phase at a distance of 1 mm from the sample surface.

The tungsten plate (variant 1) and the tantalum boat (variant 2) in the reactor were electrically heated. The linear heating rate was varied between 50 and 275 K/s. The heater temperature was measured with a Chromel–Copal thermocouple 50 μm in diameter welded to the central part of the heater. The carrier gas (argon) flow rate in the reactor was 5 cm^3/s (normal conditions). In most experiments, the initial temperature of the 5-AT sample was ~150–200°C due to the flowing carrier gas heated to this temperature. The sample was usually kept for 10–30 s at an elevated temperature that did not exceed its melting point. The 5-AT decomposition products were sampled with a quartz probe with an internal cone angle of 40° and an inlet hole diameter of 70 μm. The hole was placed at a distance of ~2–3 mm from the heater. To avoid the clogging of the probe hole with condensed products of 5-AT decomposition, the probe end was heated to ~300°C using a electrically heated wire coiled on its end [21].

The main principle of DMSTA is that the detected peak intensities (I_i) in the mass spectrum of the sample taken at the outlet of the reactor are directly proportional to the rates of formation of the corresponding decomposition products (w_i):

$$w_i = W_{\mathrm{Ar}} \frac{I_i}{I_{\mathrm{Ar}}} \frac{1}{A_i}, \quad (1)$$

where A_i is the calibration coefficient, and I_{Ar} and W_{Ar} are the intensity of the mass peak of Ar and the volume flow rate of argon, respectively [19].

The simultaneous measurement of the time dependences of the sample temperature and the peak intensities of the decomposition products makes it possible to study the decomposition kinetics. The rate of decomposition product formation under the assumption that the reaction is first-order is expressed as

$$w = \frac{\mathrm{d}x}{\mathrm{d}t} = k(1 - x), \quad (2)$$

where x is the fraction of the corresponding product formed to the moment t, which was determined as

$$x(t) = \int_0^t I_i \mathrm{d}t \Big/ \int_0^\infty I_i \mathrm{d}t, \quad (3)$$

and k is the rate constant of the reaction:

$$k = k_0 \exp(-E_a/RT). \quad (4)$$

Processing of the experimental dependences of the mass peak intensities corresponding to the ith product in the Arrhenius coordinates allows one to determine the activation energy and preexponential factor of the rate constant of the reaction yielding this product.

The decomposition products were identified using the mass spectra of individual substances obtained from the calibration experiments (NH_3, HCN, NH_2CN, and N_2) and the mass spectra taken from a database [22] (HN_3, 5-AT, and melamine). The calibration coefficients for individual substances were used to calculate the molar fractions of the decomposition products. For HN_3, melamine, and 5-AT vapor, the calibration coefficients were calculated from the material balance equation. In calibration experiments, the amount of a gaseous product introduced into the carrier gas flow was 10%. Calibration for NH_2CN was carried out by sublimation if its crystals (Cyanamide 99%, Aldrich, CAS Number 420-04-2).

RESULTS AND DISCUSSION

The intensity of 17 mass peaks in the m/e range from 2 to 126 was measured. The intensities were normalized to the maximum intensity of the m/e = 28 peak (Tables 1, 2). The average mass spectrum of the 5-AT decomposition products obtained at the moment of the maximum intensity of the m/e = 28 peak and, for comparison, data available from the literature [9] are presented in Table 1. The intensity ratios between most mass peaks observed in this study differ markedly from those observed previously [9]. This is most likely due to the use of different experimental procedures (decomposition in a closed ampule [9] and in a flow reactor in our experiments), resulting in the formation of different decomposition products and, accordingly, different mass spectra. However, the m/e = 28 and 43 peaks remain the most intense in the mass spectrum. The peaks intensities that were not measured in [9] are given in Table 2. The m/e = 85 and

Table 1. Average mass spectrum of the products of 5-AT thermal decomposition at the moment of the maximum intensity of $m/e = 28$ compared with literature data (variant 1)

m/e	14	15	16	17	26	27	28	29	30	42	43	44
I, %*	5.2	5.7	12.9	14.8	3.1	16.4	100	7.2	3.0	17.6	71.0	8.2
I, % [9]	1.7	24.2	2.2	5.5	1.7	3.8	100	27.7	1.9	16.8	100	4.2

* Data of the present work.

126 peaks are due to the vapor of 5-AT and melamine, and the $m/e = 41$, 55, and 57 peaks are probably due to the nitrileimine species (CH_3N_3, structural formula $NH_2{-}C^{-}{=}N^{+}{=}NH$) [9, 17], which can be formed from the 5-AT molecule via the elimination of N_2.

Seven products resulting from the thermal decomposition of 5-AT were identified: HN_3, N_2, NH_2CN, HCN, NH_3, melamine, and 5-AT vapor. The same products were identified earlier [7, 8] by IR spectroscopy at a sample heating rate of 100 K/s. However, the decomposition kinetics at high heating rates was not studied [7, 8].

The typical time dependences of the mass peak intensities for the products of 5-AT decomposition (variant 1) at a heating rate of ~135 K/s and T_0 ~ 155°C are shown in Fig. 2. The mass peak intensities minus the contributions from the fragment peaks of other products are presented here. 5-AT decomposition products appear above the melting point of 5-AT, and the first product detected is HN_3. The formation of N_2, NH_2CN, HCN, and 5-AT vapor is also observed at this stage. Melamine formation begins at 305°C (350°C [8]). The second maximum of formation of the products N_2, NH_2CN, and HCN is observed above 400°C, whereas no 5-AT vapor is detected at this temperature. Thus, it can be assumed that the first maximum arises from the decomposition of 5-AT and the second maximum is due to reactions involving only the secondary products of 5-AT decomposition.

The time dependences of the intensities of the $m/e = 28$ peak (with the contributions from the other products not taken into account) at different heating rates are plotted in Fig. 3. As was shown above, the dependences have two maxima. The sample was heated to different final temperatures (from 360 to 620°C). When the final temperature did not exceed 500°C (heating rates below 100 K/s), the second maximum was faint or was not observed at all. Similar regularities were observed for the time dependences of the $m/e = 17$, 27, and 42 peak intensities. Thus, the first stage of the thermal decomposition of 5-AT ($T <$ 500°C) most likely yields secondary products of 5-AT, which are thermally stable substances (for example, melem (Fig. 1, structure **5**) [10]). Below 500°C, these substances do not pass into the gas phase (remain in the condensed phase on the substrate) and can substantially change the elemental composition of the products formed at the first stage of 5-AT decomposition as compared to the initial composition.

Table 2. Intensities of the $m/e = 41$, 55, 57, 85, and 126 peaks in the average mass spectrum of the products of 5-AT thermal decomposition normalized to the intensity of the m/e = 28 peak at the moment of its maximum (variant 1)

m/e	41	55	57	85	126
I, %	19.3	6.4	12.5	7.1	15.9

In all experiments at different heating rates, the $m/e = 43$ peak (HN_3) had a single maximum coinciding with the first maximum of the $m/e = 28$ peak intensity. Thus, the experimentally observed stepwise character of the thermal decomposition of 5-AT is due to the decomposition of 5-AT itself at the first stage and reactions involving only secondary products at the second stage.

The composition of the 5-AT thermal decomposition products minus melamine (at the instant the first intensity maximum of the $m/e = 28$ peak is reached) at different heating rates and different initial temperatures is presented in Table 3 (variant 1). The major products are HN_3 and N_2. It can be seen that their mole fraction is ~0.75 of the total amount of the gaseous products and is almost independent of the heating rate. The concentrations of the other products (NH_2CN, HCN, NH_3, 5-AT vapors) are scattered, which is likely due to the reactions involving NH_2CN in the condensed phase (polymerization, decomposition, and others) proceeding to different extents. Melamine was not detected in some experiments.

The overall 5-AT thermal decomposition reaction taking into account melamine ($C_3H_6N_6$) is given below (T ~ 355°C, heating rate of ~135 K/s):

$$CH_3N_5(\text{5-AT}) \longrightarrow 0.95HN_3 + 0.53N_2 + 0.23NH_2CN + 0.12NH_3 + 0.1C_3H_6N_6 + 0.09HCN + 0.03CH_3N_5. \quad \text{(V)}$$

The amounts of elements in the gaseous products of 5-AT decomposition formed at the first stage suggest the empirical formula $C_{0.65}H_{2.55}N_{5.33}$. The maximum deviation of the material balance from the initial one is observed for C and is 35%, whereas for H and N it is 15 and 11%, respectively. As was noted above, the cause of the material imbalance for the elements is probably due to the formation of thermally stable compounds (presumably, melem $C_6H_6N_{10}$) in the

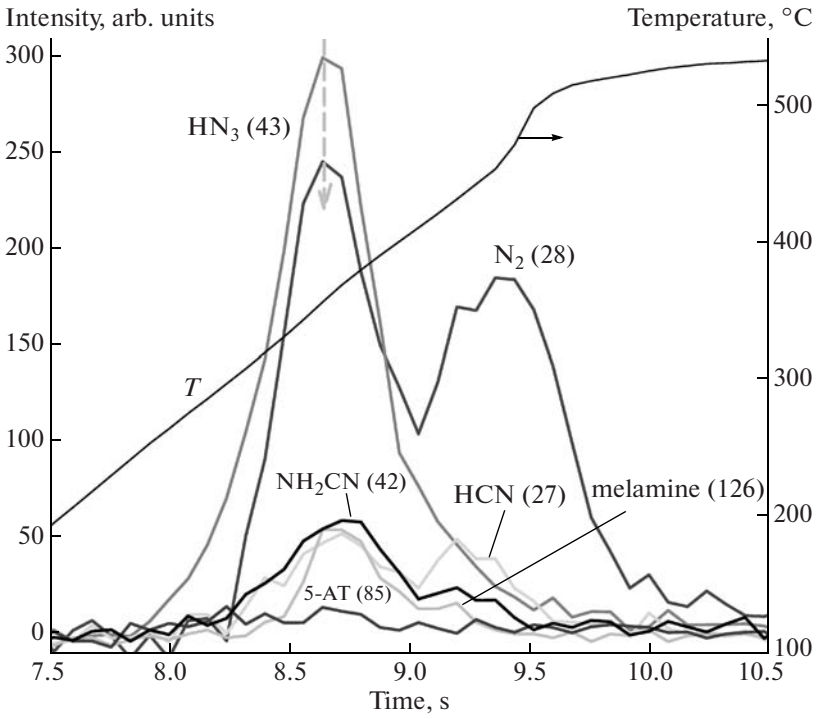

Fig. 2. Typical time dependences of the mass peak intensities of the 5-AT decomposition products and of the temperature. Heating rate, ~135 K/s; T_0 ~ 155°C; variant 1.

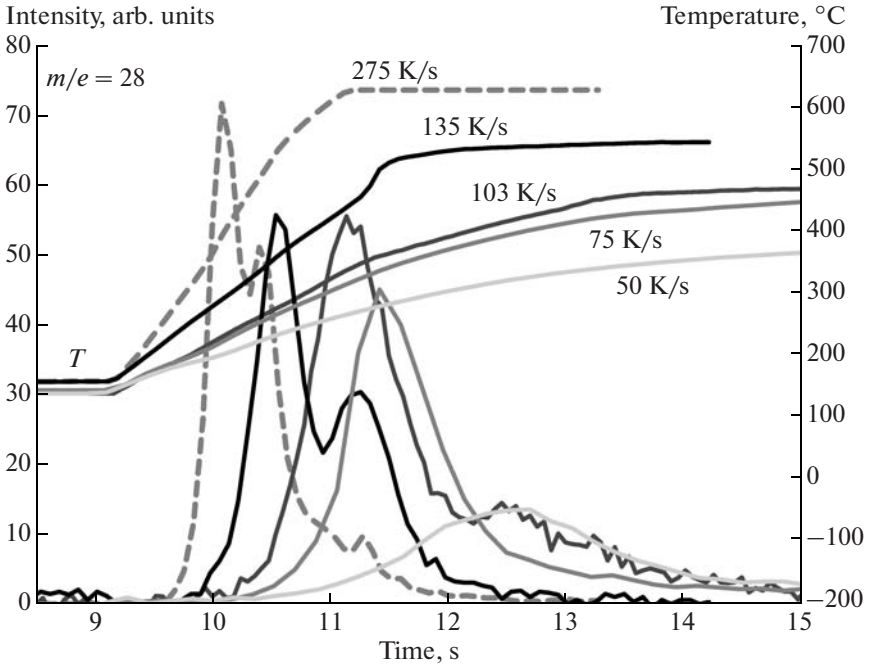

Fig. 3. Time dependences of the $m/e = 28$ peak intensity at different 5-AT heating rates (variant 1).

condensed phase, which remain on the substrate of the evaporator. According to the empirical formula of the condensed residue ($C_nH_{1.29n}N_{1.97n}$) calculated from the gas phase composition, the C/H/N ratio is 1 : 1.29 : 1.91 and is close to that for melem (1 : 1 : 1.67) within 30% error.

At a heating rate higher than 160 K/s, the decomposition of 5-AT (variant 2) occurs with the short-lived ignition of the gaseous products (the bright red flash with the duration shorter than 0.04 s—result of video filming). Most likely, this behavior is due to the accumulation of hydrogen azide in the weakly blown cell

Table 3. Composition of the products (in mole fractions) of 5-AT thermal decomposition at the moment of the maximum intensity of the nitrogen peak ($m/e = 28$) at different heating rates and initial temperatures (variant 1)

dT/dt, K/s	T_0, °C	HN_3	N_2	NH_2CN	HCN	NH_3	5-AT vapor
75	195	0.49	0.20	0.05	0.09	0.08	0.09
110	200	0.50	0.29	0.04	0.06	0.04	0.07
135	155	0.48	0.27	0.12	0.04	0.06	0.01
260	150	0.47	0.28	0.05	0.08	0.08	0.04
275	160	0.50	0.24	0.08	0.07	0.07	0.04
Average value		0.48 ± 0.02	0.25 ± 0.05	0.07 ± 0.05	0.07 ± 0.03	0.06 ± 0.03	0.05 ± 0.04

followed by exothermic decomposition. The gas temperature ~1–2 mm away from the sample at the flash point changed from 300 to ~1000°C. In mass spectrometric experiments during the flash in the gas phase, which can also be judged from the sharp change in the heater temperature (Fig. 4) at the temperature point of ~335°C, the products with masses of 17 (NH_3), 27 (HCN), 28 (N_2), 41 (fragment ion HCN_2^+ from CH_3N_3), and 42 (NH_2CN) formed at high rates. The increase in the above listed peaks is arises from the additional heating of the tantalum boat and sample due to the exothermic decomposition of the resulting hydrogen azide in the gas phase. The intensity of the $m/e = 28$ peak (N_2) changed considerably, and the

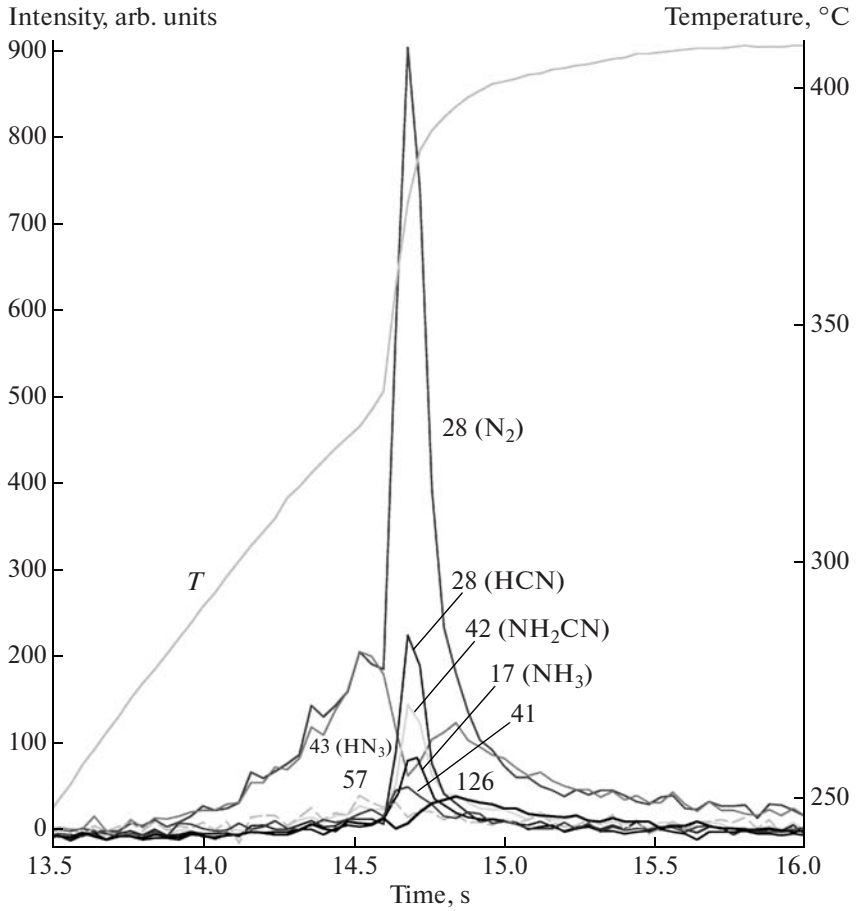

Fig. 4. Dependences of the mass peak intensities of the products of 5-AT decomposition with a flash. The heating rate is 157 K/s (variant 2).

intensity of the m/e = 43 peak (HN_3) decreased (Fig. 4). The thermal decomposition of hydrogen azide proceeds via the overall reaction [23]

$$3HN_3 \longrightarrow NH_3 + 4N_2. \quad \text{(VI)}$$

The composition of the gaseous products before the flash and at the flash point normalized to 1 mol at different gas temperatures is given in Table 4. At the flash point, 0.3 mol of nitrogen and 0.08 mol of ammonia were formed. The ratio between the amounts of N_2 and NH_3 formed from hydrogen azide was ~3.8, which is close to the ratio $N_2/NH_3 = 4$ in the products of reaction (VI).

Thus, it was shown that hydrogen azide resulting from the thermal decomposition of 5-AT decomposes with heat evolution, which intensifies the decomposition of the starting sample. The heat evolution is not due to the combustion of 5-AT, because the substance does not burn by itself under these conditions. Probably, this process can occur during the self-sustained combustion of 5-AT at high pressures.

Calculation of the Kinetic Parameters of the Primary Stages of 5-AT Thermal Decomposition

The decomposition of the 5-AT molecule can proceed via two routes to form HN_3 (reactions (I), (II), and (III)) and N_2 (reaction (IV)).

The typical time dependences of the mass peak intensities of the 5-AT decomposition products (NH_2CN and HN_3) are shown in Fig. 5. The intensity of the $m/e = 42$ peak (NH_2CN) amplified to the maximum intensity of the $m/e = 43$ peak (HN_3) is shown as a dashed line for comparison. The initial point and maximum of the NH_2CN peak coincide in time satisfactorily with those of the HN_3 peak at heating rates below 160 K/s. The similar behaviors of the HN_3 and NH_2CN mass peaks is due to reaction (I), (II), or (III). According to this reaction, the decomposition products are formed in equal amounts. However, the observed mole fraction of HN_3 exceeds that of NH_2CN by a factor of 4–10. This discrepancy can be due to the fact that NH_2CN participates in secondary reactions in the condensed phase [7, 9, 10].

Table 4. Temperature of the gas phase and the composition of the gaseous products (in mole fractions) for 5-AT thermal decomposition before and after the flash point (variant 2)

T, °C	HN_3	N_2	HCN	NH_3	NH_2CN
~330	0.73	0.27	–	–	–
~1000	0.09	0.57	0.19	0.08	0.07

The rate constant of 5-AT thermal decomposition for the first route was calculated from the concentration profile of each component (HN_3 and NH_2CN) formed in this reaction, and the rate constant for the second route was calculated from the N_2 concentration profile only.

The dependence of $\log\left(\frac{dx}{dt}\frac{1}{(1-x)}\right)$ on $1/T$ for the rate constant of formation of each product is linear at $0 < x < 0.5$ (Fig. 6), indicating that the formation of

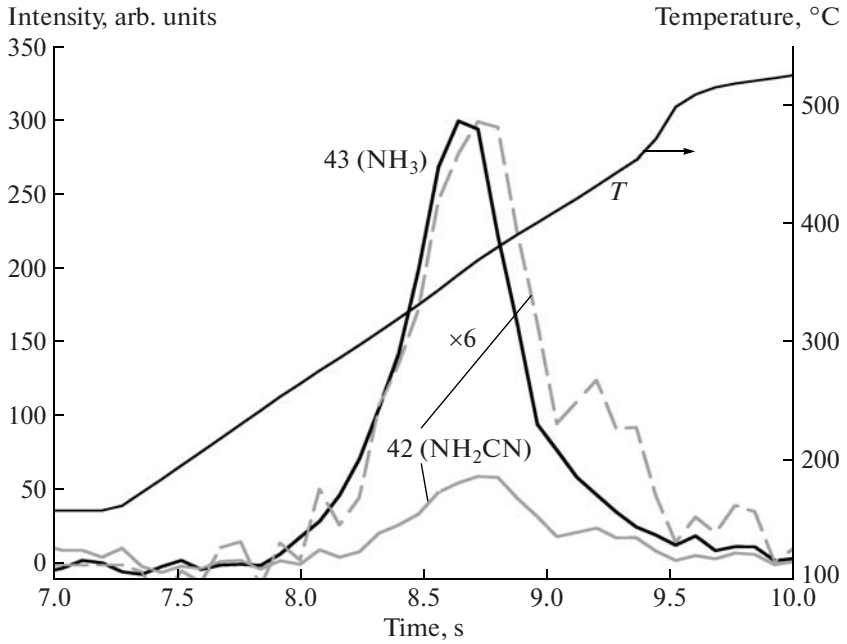

Fig. 5. Time dependences of the $m/e = 42$ (NH_2CN) and 43 (HN_3) peak intensities for 5-AT decomposition products (taking into account the contributions from other substances to these peaks). The amplified intensity of the $m/e = 42$ (NH_2CN) peak is shown as a dashed line. The heating rate is 135 K/s, and the initial temperature of the sample is 155°C (variant 1).

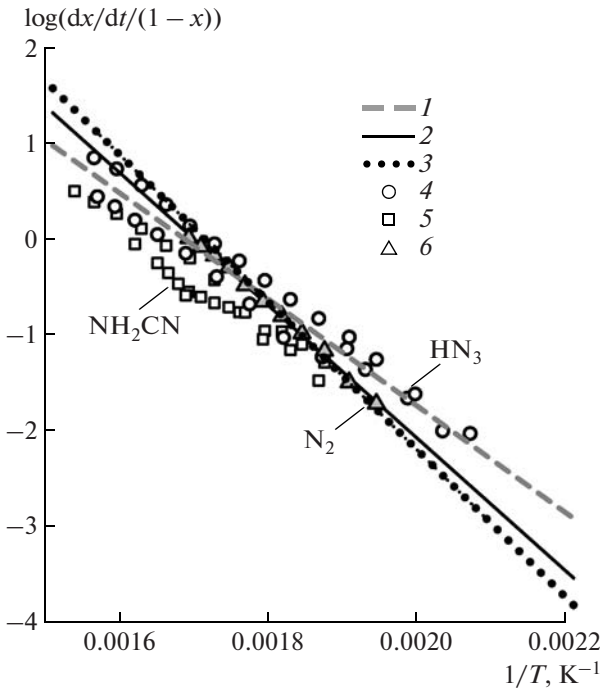

Fig. 6. Temperature dependences of the rate constants of 5-AT thermal decomposition in the Arrhenius coordinates: (*1*) average value of the rate constant of decomposition via route 1 ($CH_3N_5 \longrightarrow HN_3 + NH_2CN$) (this work), (*2*) the same for route 2 ($CH_3N_5 \longrightarrow N_2 + CH_3N_3$) (this work), (*3*) published data [10], and (*4–6*) the rate constants of 5-AT thermal decomposition calculated from the concentration profiles of (*4*) HN_3, (*5*) NH_2CN, and (*6*) N_2.

these products is a first-order reaction, in agreement with the literature [9, 10].

The values of E_a and $\log k_0$ for the rate constant of 5-AT thermal decomposition for two different decomposition routes are presented in Table 5, where they are compared with literature data [10]. The calculation was performed for a 5-AT conversion (extent of formation of the product) of $x < 0.5$ between 205 and 380°C, where the primary reactions of 5-AT decomposition most probably occur and the secondary reactions exert only a weak effect on the rate of decomposition product formation. The kinetic parameters of the rate constant of 5-AT thermal decomposition via the first route calculated from the HN_3 and NH_2CN formation rates are similar. The average values of the activation energy and logarithm of the preexponential factor in the rate constant of 5-AT decomposition via the first route ($CH_3N_5 \longrightarrow HN_3 + NH_2CN$) are 107.2 ± 12.0 kJ/mol and $\log k_0 = 9.2 \pm 1.2$ s^{-1}, whereas those for the second route ($CH_3N_5 \longrightarrow N_2 + CH_3N_3$) are 132.2 ± 5.1 kJ/mol and $\log k_0 = 11.7 \pm 0.8$ s^{-1}. The calculated kinetic parameters (E_0 and $\log k_0$) of 5-AT decomposition via the first route are lower than the literature values [10]. According to the mechanism of 5-AT thermal decomposition [9], the decomposition of the imino form of 5-AT, which prevails below the melting point, proceeds via tetrazole ring splitting to yield HN_3 and NH_2CN (route 1). Upon melting/evaporation, the imino form of 5-AT turns into the amino form [9], which also decomposes via tetrazole ring splitting to give N_2. Thus, it can be assumed that, for 5-AT decomposition at low heating rates [9, 10] above the melting point, the rate constant of 5-AT decomposition is determined by the parameters of amino form decomposition via route 2 with the formation of N_2. This assumption is consistent with the fact that the kinetic parameters (route 2) obtained in our work ($E_a = 132.2 \pm 5.1$ kJ/mol, $\log k_0 = 11.7 \pm 0.8$ s^{-1}) are close to published data [10] ($E_a = 147.0 \pm 10.0$ kJ/mol, $\log k_0 = 13.1 \pm 1.0$ s^{-1}). Thus, the thermal decomposition of 5-AT at high heating rates with the simultaneous detection of the resulting decomposition products made it possible to distinguish two routes of 5-AT decomposition and to determine their kinetic parameters. The rate constants of 5-AT thermal decomposition calculated for the two different decomposition routes are presented in the Arrhenius coordinates in Fig. 6 and are compared with published data [10].

Table 5. The values of E_a and $\log k_0$ of the thermal decomposition of 5-AT (for the two different decomposition routes) compared with published data

Calculation variant	Product	E_a, kJ/mol	$\log k_0$ [s^{-1}]
Route 1	HN_3	108.6 ± 8.7	9.5 ± 0.9
	NH_2CN	105.7 ± 11.2	8.9 ± 0.9
Route 2	N_2	132.2 ± 5.1	11.7 ± 0.8
[10]	–	147.0 ± 10	13.1 ± 1.0

The activation energy obtained by us for route 1 (107.2 ± 12.0 kJ/mol) is close to that (99.5 kJ/mol) obtained previously [14], is equal to the energy necessary for the splitting of the tetrazole ring of 5-AT, and differs substantially from the published value of 200 kJ/mol [13]. Thus, HN_3 and NH_2CN (route 1) do not form via the simultaneous splitting of two bonds in the tetrazole ring, contrary to what was suggested earlier [13]. Their formation proceeds via the splitting of the tetrazole ring of the imino form of 5-AT followed by the detachment of HN_3 [9].

The route of 5-AT decomposition is determined by the tautomeric form of 5-AT. Using the ratio between the HN_3 and N_2 concentrations (2 : 1, Table 3) in the products of 5-AT decomposition formed via the two decomposition routes, one can estimate the ratio between the concentration of the tautomeric forms in the 5-AT sample (the imino form content is two times higher than the amino form content) and, accordingly,

the ratio between the amounts of the products formed via the two routes at high heating rates:

$$\text{5-AT} \longrightarrow 2/3\ (HN_3 + NH_2CN) + 1/3\ (N_2 + CH_3N_3). \quad \text{(VII)}$$

CONCLUSIONS

The kinetics of 5-AT thermal decomposition in the condensed phase at high heating rates (~100 K/s) was studied by the dynamic mass spectrometric thermal analysis using a molecular beam sampling system, and the product composition was determined. Seven products formed upon the thermal decomposition of 5-AT were identified: HN_3, N_2, NH_2CN, HCN, NH_3, melamine, and 5-AT vapor. Two routes of 5-AT decomposition yielding HN_3 and NH_2CN (route 1) and N_2 and CH_3N_3 (route 2) were distinguished. The kinetic parameters (activation energies and rate constants of 5-AT thermal decomposition) were determined for each route.

It was shown that hydrogen azide formed under certain conditions of 5-AT thermal decomposition decomposes with heat evolution, which intensifies the decomposition of the starting sample. This process can occur during the self-sustained combustion of 5-AT at elevated pressures.

The data obtained can be used for the further improvement of the detailed kinetic mechanism of the thermal decomposition and combustion of tetrazole compounds.

ACKNOWLEDGMENTS

This work was supported in part by the Research Office of the US Army (grant no. W911NF-05-1-0549).

REFERENCES

1. Kozyro, A.A., Simirskii, V.V., Krasulin, A.P., et al., *Zh. Fiz. Khim.*, 1990, vol. 64, no. 3, p. 656.
2. Neidert, J.B., Black, R.E., Lynch, R.D., et al., *Propulsion Conf.*, Cleveland, Ohio, 1998, vol. 2, p. 77.
3. Fallis, S., Reed, R., Lu, Y.-C., et al., *Proc. Halon Options Technical Working Conf.*, Gaithersburg, Md.: NIST, 2000, p. 361.
4. Wierenga, P.H. and Holland, G.F., *Proc. Halon Options Technical Working Conf.*, Gaithersburg Md.: NIST, 1999, p. 453.
5. Lesnikovich, A.I., Sviridov, V.V., Gaponik, P.N., et al., *Dokl. Akad. Nauk BSSR*, 1985, vol. 29, no. 3, p. 824.
6. Fogel'zang, A.E., Egorshev, V.Yu., Sinditskii, V.P., et al., *Mater'yaly IX Vses. simp. po goreniyu i vzryvu* (Proc. IX All-Union Symp. on Combustion and Explosion), Chernogolovka, Moscow oblast, 1989, p. 3.
7. Brill, T.B. and Ramanathan, H., *Combust. Flame*, 2000, vol. 122, p. 165.
8. Oyumi, G.Y. and Brill, T.B., *Combust. Flame*, 1991, vol. 83, p. 345.
9. Levchik, S.V., Ivashkevich, O.A., Balabanovich, A.I., et al., *Thermochim. Acta,* 1992, vol. 207, p. 115.
10. Lesnikovich, A.I., Ivashkevich, O.A., Levchik, S.V., et al., *Thermochim. Acta*, 2002, vol. 388, p. 233.
11. Brill, T.B., *Prog. Energy Combust. Sci.*, 1992, vol. 18, p. 91.
12. Cronin, J.T. and Brill, T.B., *Appl. Spectrosc.*, 1987, vol. 41, no. 7, p. 1147.
13. Jian-Guo Zhang., Li-Na Feng, Shao-Wen Zhang., and Tong-Lai Zhang., *J. Mol. Model.*, 2008, no. 14, p. 403.
14. Chen, Z. and Xiao, H., *Int. J. Quantum Chem.*, 2000, vol. 79, p. 350.
15. Shurukhin, Yu.V., Klyuev, N.A., and Grandberg, I.I., *Khim. Geterotsikl. Soedin.*, 1982, no. 6, p. 723.
16. Reimlinger, H., *Chem. Ind.*, 1972, p. 294.
17. Brady, L.E., *J. Heterocycl. Chem.*, 1970, vol. 21, p. 1223.
18. Korobeinichev, O.P., Kuibida, L.V., Paletsky, A.A., and Shmakov, A.G., *J. Propul. Power*, 1998, vol. 14, no. 6, p. 991.
19. Korobeinichev, O.P., *Fiz. Goreniya Vzryva*, 1987, vol. 23, no. 5, p. 64.
20. US Patent 5594146, 1997.
21. Tereshenko, A.G., Korobeinichev, O.P., Paletsky, A.A., et al., *Proc. 8th Int. Workshop on Combustion and Propulsion*, Arzago d'Adda, Italy, 2002, p. 15.
22. *NIST Chemical Webbook*, http://webbook.nist.gov/chemistry/.
23. Rozenberg, A.S., Arsen'ev, Yu.N., and Voronkov, V.G., *Fiz. Goreniya Vzryva*, 1970, vol. 6, no. 3, p. 302.